◆ Human Brain Mapping 37:165–178 (2016) ◆

Essential Tremor Is Associated With Disruption of Functional Connectivity in the Ventral Intermediate Nucleus—Motor Cortex—Cerebellum Circuit

Weidong Fang,[1]* Huiyue Chen,[1] Hansheng Wang,[1] Han Zhang,[2] Munankami Puneet,[1] Mengqi Liu,[1] Fajin Lv,[1] Tianyou Luo,[1] Oumei Cheng,[3] Xuefeng Wang,[3] and Xiurong Lu[3]

[1]Department of Radiology, The First Affiliated Hospital of Chongqing Medical University, Chongqing, China
[2]Center for Cognition and Brain Disorders, Hangzhou Normal University, Hangzhou, China
[3]Department of Neurology, the First Affiliated Hospital of Chongqing Medical University, Chongqing, China

Abstract: The clinical benefits of targeting the ventral intermediate nucleus (VIM) for the treatment of tremors in essential tremor (ET) patients suggest that the VIM is a key hub in the network of tremor generation and propagation and that the VIM can be considered as a seed region to study the tremor network. However, little is known about the central tremor network in ET patients. Twenty-six ET patients and 26 matched healthy controls (HCs) were included in this study. After considering structural and head-motion factors and establishing the accuracy of our seed region, a VIM seed-based functional connectivity (FC) analysis of resting-state functional magnetic resonance imaging (RS-fMRI) data was performed to characterize the VIM FC network in ET patients. We found that ET patients and HCs shared a similar VIM FC network that was generally consistent with the VIM anatomical connectivity network inferred from normal nonhuman primates and healthy humans. Compared with HCs, ET patients displayed VIM-related FC changes, primarily within the VIM-motor cortex (MC)-cerebellum (CBLM) circuit, which included decreased FC in the CBLM and increased FC in the MC. Importantly, tremor severity correlated with these FC changes. These findings provide the first evidence that the pathological tremors observed in ET patients might be based on a physiologically pre-existing VIM - MC - CBLM network and that disruption of FC in this physiological net-

Additional Supporting Information may be found in the online version of this article.

Contract grant sponsor: Natural Science Foundation of Chongqing; Contract grant number: cstc2014jcyjA10047; Contract grant sponsor: Medicine Scientific Key Research Project of Chongqing Health Bureau (Project No. 2010-2-030); Contract grant sponsor: National Natural Science Foundation of China; Contract grant number: Contract grant number: 81201156

*Correspondence to: Weidong Fang, Department of Radiology, The First Affiliated Hospital of Chongqing Medical University, No. 1 Youyi Road, Yuzhong District, Chongqing 400016, China. E-mail: fwd9707@sina.com

Received for publication 4 October 2014; Revised 5 September 2015; Accepted 28 September 2015.

DOI: 10.1002/hbm.23024
Published online 15 October 2015 in Wiley Online Library (wileyonlinelibrary.com).

work is associated with ET. Further, these findings demonstrate a potential approach for elucidating the neural network mechanisms underlying this disease. *Hum Brain Mapp 37:165–178, 2016.*

Key words: essential tremor; functional connectivity; resting state; functional magnetic resonance imaging; cerebellum; thalamus; motor cortex; ventral intermediate nucleus

INTRODUCTION

Essential tremor (ET), the most prevalent movement disorder in adults [Li et al., 1985; Louis and Ferreira, 2010], is commonly considered to be caused by the activity of a central tremor network [Brittain et al., 2015; Raethjen and Deuschl, 2012]. However, little is known about the tremor network and its underlying pathogenesis [Elias and Shah, 2014; Louis, 2014]. The ventral intermediate nucleus (VIM) of the thalamus has been introduced as a target to alleviate tremors via several treatment methods, including thalamotomy [Hassler and Riechert, 1954], stereotactic thalamotomy [Zirh et al., 1999], deep-brain stimulation (DBS) [Klein et al., 2012; Papavassiliou et al., 2008], gamma knife radiosurgery [Kooshkabadi et al., 2013], and focused ultrasound [Elias et al., 2013]; these treatments have achieved good therapeutic responses in ET patients. These results suggest that the VIM can be considered as a seed region to study the central tremor network in ET.

Invasive tract-tracing studies [Asanuma et al., 1983a; Yamamoto et al., 1983] of normal nonhuman primates have shown that the VIM connects with the motor cortex (MC) and the cerebellum (CBLM) and that these connections form a VIM - MC - CBLM anatomical connectivity network. A similar VIM anatomical network has been detected in healthy humans using a non-invasive tract-tracing method termed diffusion tensor imaging (DTI) [Behrens et al., 2003; Johansen-Berg et al., 2005; Kincses et al., 2012]. Importantly, DTI studies have revealed that anatomical network modulations primarily occur within this circuit in ET patients after DBS [Klein et al., 2012] or focused ultrasound therapy [Wintermark et al., 2014]. This evidence suggests that the VIM anatomical network is associated with tremors in ET patients. However, brain activity data supporting this result is as yet unknown. Studies of electroencephalography or magnetoencephalography combined with electromyography have shown that local field potential changes primarily occur in the VIM - MC - CBLM circuit when normal nonhuman primates [Yamamoto et al., 1983] and healthy humans [Pollok et al., 2004] perform a physiological tremor task or when ET patients have undergone DBS therapy [Connolly et al., 2012]. Additionally, PET [Perlmutter et al., 2002] and task-evoked fMRI [Hesselmann et al., 2006] studies have revealed that cerebral blood flow responses and blood oxygen level-dependent signals representing brain activation primarily occur in the same circuit when ET patients have undergone DBS therapy. However, these methods only measure regional brain area activity, and the network mechanisms underlying this activity remain unclear.

Functional connectivity (FC) analysis of resting-state functional magnetic resonance imaging (RS-fMRI) has been suggested as a promising method to study the neural network mechanisms underlying movement disorders, such as Parkinson's disease (PD) [Helmich et al., 2011; Kahan et al., 2014], Huntington's disease [Werner et al., 2014] and ET [Fang et al., 2013; Popa et al., 2013]. Using this method, an FC network similar to the VIM anatomical network composed of the VIM - MC - CBLM circuit has been described in healthy humans in several studies [Anderson et al., 2011; Zhang et al., 2008]. Furthermore, using FC analysis of RS-fMRI data, Helmich et al. [2011] have reported that pallidal dysfunction drives the VIM - MC - CBLM circuit to generate tremors in PD, another disease with tremor symptoms. However, to the best of our knowledge, the use of resting-state FC (RS-FC) to study the VIM-related network in ET patients has not been previously reported.

We hypothesized that RS-FC analysis would reveal a similar VIM - MC - CBLM FC network in ET patients to the FC network reported in previous studies and that internal FC changes in this network would underlie the pathological tremors observed in ET patients. To test this hypothesis, we constructed VIM FC maps at the whole-brain level for ET patients and healthy controls (HCs). Moreover, we performed within-group, inter-group and imaging results-behavior correlation analyses to reveal VIM-related RS-FC network features in ET patients.

MATERIALS AND METHODS

Subjects

We recruited 35 nondementia ET patients and 29 HCs, all of whom were right-handed. This dataset has not been used in any of our previous studies [Fang et al., 2013; Sheng et al., 2014]. Each subject signed an informed consent form approved by the Ethics Committee of The First Affiliated Hospital of Chongqing Medical University (Chongqing, China), and the study was performed in accordance with the Declaration of Helsinki of the World Medical Association. All patients met the diagnosis of definite ET according to the Movement Disorders Consensus Criteria [Deuschl et al., 1998], which include the presence of bilateral, visible, persistent, and largely symmetric postural or kinetic tremors involving the hands and forearms

TABLE I. Demographic and clinical features of ET patients and HCs

Measure	ET	HCs	*P*-value
Demographic			
Age	47.3 ± 11.3	43.4 ± 14.4	0.28
Gender (male: female)	19:7	19:7	1
Handedness (right: left)	26:0	26:0	1
Clinical			
Age of onset (years)	34.3 ± 13	NA	
Disease duration (years)	12.9 ± 7.2	NA	
Positive family history	11	NA	
History of alcohol to alleviate symptoms		NA	
Positive	5	NA	
Negative	7	NA	
NA	14	NA	
Pattern appearance of tremor		NA	
Kinetic	26	NA	
Postural	19	NA	
Rest	5	NA	
Intention	2	NA	
Left and Right hand tremor situation		NA	
Bilateral and right = left	19	NA	
Bilateral and right > left	3	NA	
Bilateral and right < left	2	NA	
Unilateral only right	2	NA	
Unilateral only left	0	NA	
The Fahn-Tolosa-Marin TRS		NA	
TRS-parts A&B	12.7 ± 7.2	NA	
TRS-part C	7.7 ± 4.0	NA	
Neuropsychological			
MMSE	26.0 ± 1.5	27.0 ± 2.1	0.35
Hospital Anxiety and Depression Scale (HAD)	8.30 ± 5.3	7.27 ± 5.1	0.54
HAD-A	4.23 ± 2.5	3.61 ± 2.7	0.16
HAD-D	4.07 ± 2.8	3.66 ± 2.4	0.27

ET: essential tremor; HCs: healthy controls; NA: not applicable; MMSE: mini mental state examination; HAD-A: hospital anxiety and depression scale-anxiety party; HAD-D: hospital anxiety and depression scale-depression party.

for at least five years. The exclusion criteria were the following: PD, dystonia, psychogenic tremor, thyroid disease, or any other neurological dysfunction. Nine ET patients and 3 HCs were excluded from the present study because they did not meet our quality assurance criteria (discussed below). Hence, the final subjects for this study included 26 ET patients and 26 age-, sex-, and education-matched HCs.

Clinical and Neuropsychological Assessments

All ET patients agreed to a videotaped examination to establish a clinical rating by two movement disorder specialists (X Lu and O Chen) who were blinded to the neuroimaging results. Clinical features were recorded. Postural tremors were assessed with the arms raised horizontally forward and the hands pronated. Kinetic tremors were evaluated while hand pouring, using a spoon, drinking, drawing Archimedes spirals and lines and performing the finger-nose-finger task. Intention tremor was estimated using the finger-nose-finger task. Tremor severity was assessed using the Fahn-Tolosa-Marin Tremor Rating Scale (TRS) [Fahn et al., 1993; Louis et al., 2000], which consists of motor and daily living assessments. The motor assessment included questions 1–14 (parts A&B), which address tremor severity and location and the drawing and writing functions of the hands. The daily living assessment consists of questions 15–21 (part C) and is based on patient descriptions. All subjects were screened using the Mini Mental State Examination (MMSE) [Zhang et al., 1990] to rule out dementia (MMSE < 24) and the Hospital Anxiety and Depression Scale (HADS) questionnaire [Snaith and Zigmond, 1986] to rule out depression (depression subscale score > 7) and anxiety (anxiety subscale score > 7).

All ET patients presented with mild to moderate kinetic tremors in their hands and arms as the main clinical features. To avoid medical confounders, we only used data obtained during the initial visit and under antitremor medication-naïve conditions prior to RS-fMRI examinations. There were no significant differences in the MMSE or HADS scores between the ET and HC groups. The demographic information and the clinical and neuropsychological assessment data are shown in Tables I and Supporting Information Table S1.

MAGNETIC RESONANCE IMAGING

All MR images were acquired using a GE Signa Hdxt 3-T scanner (General Electric Medical Systems, Waukesha, WI) equipped with a standard 8-channel head coil. Foam padding and earplugs were used to minimize head motion and to reduce scanner noise. During RS-fMRI scanning, all subjects were told to relax, to remain still with their eyes closed, and to remain awake (which was immediately confirmed via post-scan debriefing). RS-fMRI data were acquired using an echo-planar imaging (EPI) pulse sequence with the following parameters: 33 axial slices, slice thickness/gap = 4.0/0 mm, matrix = 64 × 64, TR = 2000 ms, TE = 40 ms, flip angle = 90°, and FOV = 240 × 240 mm. A total of 240 volumes were obtained (duration = 8 min). High-resolution 3D T1-weighted images (TR = 8.3 ms, TE = 3.3 ms, flip angle = 15°, slice thickness/gap = 1.0/0 mm, FOV = 240 × 240 mm, and matrix = 256 × 192) and T2-weighted FLAIR images (TR = 8000 ms, TE = 126 ms, TI = 1500 ms, slice thickness/gap = 5.0/1.5 mm, FOV = 240 × 240 mm, and matrix = 256 × 192) were also acquired. We did not use the T2-weighted FLAIR images for data processing, but they were used for image evaluation and data quality assessment (see Quality assurance).

Image Preprocessing

Data preprocessing was conducted using DPARSFA toolbox version 2.2 (www.restfmri.net) [Chao-Gan and Yu-Feng, 2010] and REST toolbox version 1.8 (www.restfmri.net) [Song et al., 2011]. As previously described [Bernard et al., 2014; Fang et al., 2013], data processing was composed of the following steps: (i) removal of the first 10 time points; (ii) slice timing correction; (iii) realignment for head motion (also see Quality assurance); (iv) DARTELT1 segmentation and spatial normalization based on the deformation field; (v) spatial smoothing using the Gaussian kernel with $4 \times 4 \times 4$ mm^3 full-width half-magnitude (FWHM); (vi) time series detrending and filtering (0.01–0.08 Hz), and (vii) nuisance signal regression (see Supporting Information Text S1 for details). The removal of the global mean signal (GMS) enhances the spatial specificity of FC mapping, especially for subcortical regions [Fox et al., 2009]. Therefore, we conducted all of the subsequent analyses with the GMS removed. However, other studies [Murphy et al., 2009] have shown that GMS removal induces negative connectivity and introduces additional confounding factors to the inter-group comparison. Thus, we also performed data processing without GMS removal and noted that the main results were similar (Supporting Information Fig. S1-2 and Table S2).

Quality Assurance

The T1-weighted images and the T2-weighted FLAIR images were visually inspected by an experienced neuroradiologist (F Lv or T Luo). None of the subjects displayed evident abnormalities in their gross brain structure or signals. Recently published studies [Power et al., 2012, 2013; Satterthwaite et al., 2013; Van Dijk et al., 2012] have reported that head motion induces artifacts, as well as increased short-distance correlations, and decreased long-distance correlations. Therefore, we performed the following five measurements to address head motion-related concerns: (i) ET patients who manifested head tremors as the main clinical feature were not included; (ii) any subjects with gross head movement >2.0 mm and 2.0° in the x, y, and z directions were ruled out in this study; (iii) the root mean square (RMS) head movement was calculated by condensing six head realignment parameters into a single summary statistic, and we excluded subjects with a RMS head movement greater than 0.5 mm; (iv) using the criteria suggested by Power et al. [2012], the framewise displacement (FD), which reflects instantaneous head motion, was computed, and subjects with FD > 50% of the volumes (115 volumes) were excluded from this study; and (v) two-sample t-tests were performed to explore whether there were significant differences in the RMS head movement or FD head movement between the two groups.

Six ET patients who presented with head tremor as their main clinical feature were excluded from this study. Based on visual inspection, the remaining subjects had no clearly visible head movement. However, 1 ET patient with an RMS head movement > 0.5 mm and 2 ET patients and 3 HCs with an FD head movement > 50% of the volumes were excluded from this study. The RMS and FD head movement values were 0.12 ± 0.08 and $14 \pm 5\%$ for ET patients and were 0.15 ± 0.07 and $9 \pm 6\%$, for HCs. No significant differences in RMS or FD head movement were noted between the two groups ($P = 0.26$ and 0.19, respectively).

Localization of the VIM Seed Region and RS-FC Analysis

The VIM cannot be identified on conventional MR and CT images [Anderson et al., 2011; Kincses et al., 2012; Klein et al., 2012], and its location is typically determined by individual stereotactic coordinates [Hassler and Riechert, 1954; Morel et al., 1997] or population-based stereotactic coordinates [Kincses, et al., 2012; Klein et al., 2012; Papavassiliou et al., 2008]. In contrast to the individual stereotactic coordinates of the VIM, the population-based stereotactic coordinates are derived from postoperative images and facilitate the definitive determination of its location based on MNI or Talairach coordinates; thus, the population-based stereotactic coordinates could be directly used as the seed coordinates in our study. To the best of our knowledge, Papavassiliou et al. [2008] have reported the largest sample size (37 ET patients implanted with 57 DBS electrodes who were followed up for a mean duration of 26 months) among the relevant previous studies [Kincses et al., 2012; Klein et al., 2012; Papavassiliou et al., 2008]. Hence, according to the description by Papavassiliou et al. [2008], the bilateral VIM seed region coordinates in our study were 6.3 mm anterior to the posterior commissure, 12.3 mm lateral to the midline or 10.0 mm lateral to the third ventricle. Considering that the VIM is a small nucleus with an approximate size of $2-4 \times 7-10 \times 4-6$ mm^3 [Vassal et al., 2012] and that the spatial resolution of our fMRI data was $3 \times 3 \times 3$ mm^3, we took several steps to ensure the precise localization of our VIM seeds. First, based on visual inspection, the locations of the anterior commissure, the posterior commissure and the left and right VIM seed regions were identified in the MNI coordinate system. Second, similar to Bernard et al. [2014], a single voxel representing the VIM seed was used to ensure that the seed region did not overlap with the other ventrolateral nuclei of the thalamus. Third, to avoid spatial blurring (i.e., smoothing during the preprocessing step), which would result in the loss of spatial specificity, we used a relatively smaller smoothing kernel with an FWHM of $4 \times 4 \times 4$ mm^3 and no spatial smoothing of the time course of the seed region. Finally, the seed locations in all subjects were visually inspected using the RS-fMRI data in the standardized MNI space to ensure that the seed regions were not located in regions of EPI BOLD signal loss or heavy EPI image distortion. Then, Pearson correlation analysis between the time course of the seed region and the whole-brain voxels was performed in a voxel-wise manner. Fisher's z-transformation was applied to improve the normality of these correlation

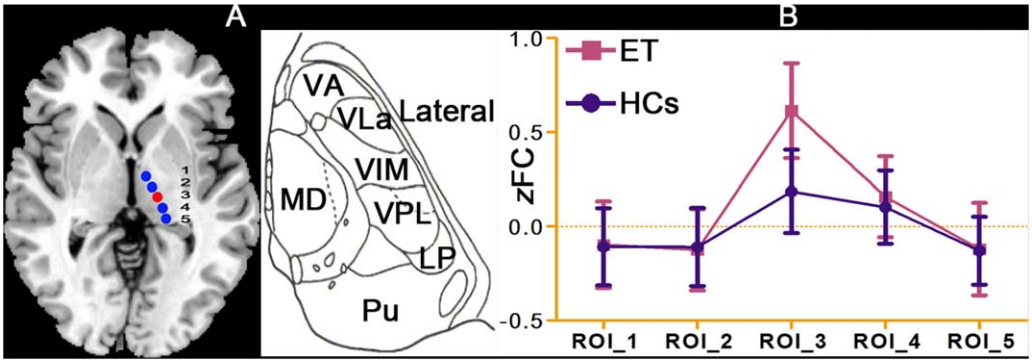

Figure 1.

Location of the seed regions in the VIM and the other four ventral lateral thalamic nuclei and spatial specificity analysis. A: According to studies conducted by Papavassiliou et al. and Morel et al., we defined the VIM seed region (red color) and the other four ventral lateral thalamus nuclei seed regions (blue color) in standardized MNI space via anatomical imaging. B: Spatial specificity analysis to determine whether the VIM seed region displayed the strongest FC with the ipsilateral primary MC among these nuclei. VIM: ventral intermediate nucleus; partial FC: partial functional connectivity; ET: essential tremor; HCs: healthy controls. [Color figure can be viewed in the online issue, which is available at wileyonlinelibrary.com.]

coefficients, and individual VIM-related RS-FC maps were constructed.

Evaluation of the Spatial Specificity of the VIM Seed Region

Although the population-based stereotactic coordinates of the VIM could be directly used as seed coordinates in our study, individual anatomical variations were present; therefore, a test to assess the spatial specificity of the VIM seed region was necessary. Previous studies [Asanuma et al., 1983b; Morel et al., 1997] have reported that the ventrolateral thalamus can be subdivided into the ventral anterior nucleus (VA), the ventral lateral anterior nucleus (VLa), the ventral lateral posterior nuclei (VLP, mainly composed of the VIM; for the nomenclature of the ventrolateral thalamus and the relationship between the VLP and the VIM, see Supporting Information Text S2), the ventral posterior lateral nucleus (VPL) and the lateral posterior nucleus (LP). Among these nuclei, the VIM displays the strongest anatomical connectivity and FC with the primary MC [Anderson et al., 2011; Hyam et al., 2012; Kincses et al., 2012]. Therefore, the test of the spatial specificity of the VIM seed region was performed using the following steps: (i) according to the atlas of the thalamus by Morel et al. [1997], we placed other seed regions of the same size as the VIM in the VA, the VLa, the VPL and the LP (Fig. 1A); (ii) we extracted the time courses of these seed regions, including that of the VIM; (iii) we performed partial correlation analysis (also referred to as a partial FC) between these seed regions and the ipsilateral primary MC (L: −42, −24, 60; R: + 42, −24, 60) [Kelly et al., 2009] (for details, see Text Supporting Information S3); and (iv) we performed mixed-effects ANOVA and two-sample *t*-tests to assess whether our VIM seed region displayed the strongest FC with the ipsilateral primary MC among these regions. A significance threshold was set at a $P < 0.05$, and Bonferroni multiple comparisons correction was performed.

Statistical Analyses

To visualize the average FC network of the left and right VIM seeds, group-specific random-effects one-sample *t*-tests were performed separately for the HCs and the ET patients with AlphaSim multiple comparison correction within a whole-brain mask, which was also implemented in AFNI software (http://afni.nimh.nih.gov/afni). The voxel-wise threshold was set at a $P < 0.05$, and the cluster threshold was set at ≥ 85 voxels (1000 Monte Carlo simulations). We combined the group-level significant brain regions into a mask, within which we further identified the group differences using the random-effects two-sample *t*-test. AlphaSim multiple comparison correction was performed within this mask. To account for the lower false-positive control effect of AlphaSim correction than that of FDR or Bonferroni correction, the voxel-wise threshold was set at $P < 0.01$, and the corrected cluster-level thresholds were obtained from 1000 Monte Carlo simulations.

Imaging Results-Behavior Correlation Analysis

Based on the two-sample *t*-test findings, the clusters with altered FC in the ET patients were identified as regions of interest (ROIs). Some of the clusters may have included multiple brain regions, and we selected a 6-mm radius spherical region located within the peak MNI coordinates as our ROI. The mean RS-FC value in each ROI was extracted for all of the ET patients, and Pearson correlation

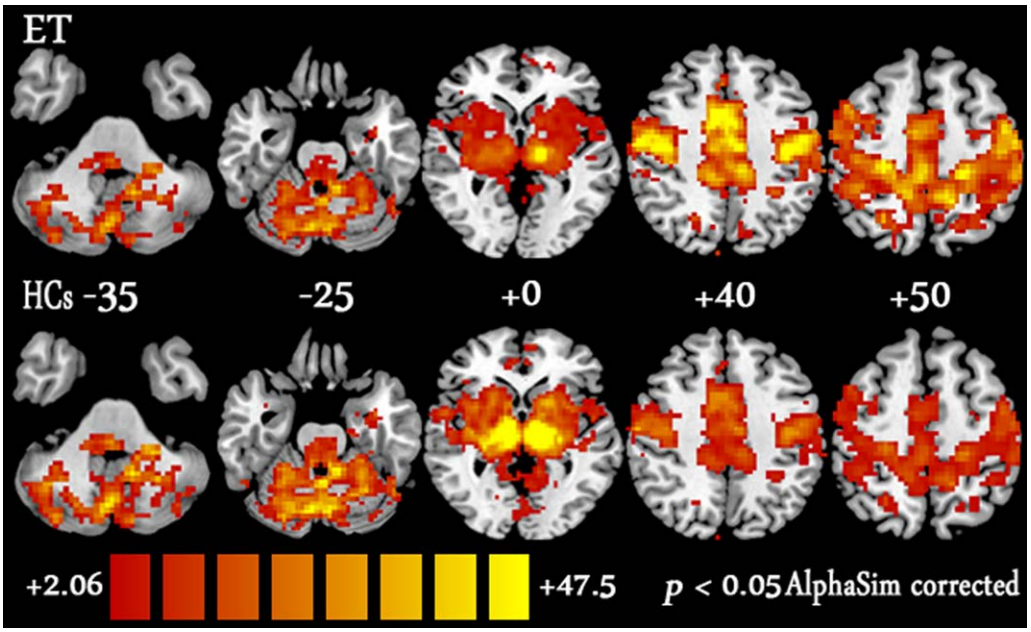

Figure 2.

Results of the one-sample *t*-test for left VIM seed region FC maps for the ET patient (upper) and HC groups (lower). The threshold was set at $P < 0.05$ with AlphaSim correction (cluster size ≥ 85 voxels, 1000 Monte Carlo simulations). The *Ch2* image depicts the underlying structure. VIM: ventral intermediate nucleus; ET: essential tremor; HCs: healthy controls. [Color figure can be viewed in the online issue, which is available at wileyonlinelibrary.com.]

coefficients were calculated between the FC values and the clinical assessment data, including the TRS parts A&B scores, the TRS part C scores, age at onset and disease duration. To improve the normality of the data, the clinical scores were converted to z scores before the correlation analyses. Kolmogorov-Smirnov tests were conducted to assess the normality of the z scores, and the results showed good normality (TRS parts A&B: $z = 0.82$, $P = 0.42$; TRS part C: $z = 0.67$, $P = 0.53$; age of onset: $z = 0.36$, $P = 0.76$; disease duration: $z = 0.61$, $P = 0.62$). Additionally, considering the relatively small sample size and the exploratory nature of this research, we used an uncorrected $P < 0.01$ rather than stringent multiple comparison correction methods such as Bonferroni correction.

Voxel-Based Morphometry (VBM) Analyses

Because brain structure is an important factor that influences RS-fMRI results, we performed VBM analysis as previously described [Bagepally et al., 2011; Lin et al., 2013]. We did not detect any significant differences in either gray matter or white matter density or volume between the ET and HC groups; these results were consistent with those of previous studies [Fang et al., 2013; Klein et al., 2012]. Therefore, these data were not taken into account as nuisance covariates in the above FC analysis.

RESULTS

VIM Seed Region FC Maps

The left VIM seed region FC maps for the ET and HC groups are shown in Figure 2. The ET patients and the HCs shared similar maps, and significantly positive FC values were observed in the CBLM (the bilateral posterior and anterior lobules, including the vermis), the MC (the bilateral primary and supplementary MC), the bilateral basal ganglia, the brainstem and the thalamus. The FC maps of the right VIM seed region were similar to those of the mirror area in the left VIM seed region and are not described here.

Group Differences

Figure 3 shows the group differences in the left VIM FC maps. Compared with HCs, ET patients exhibited decreased VIM-related FC values in the CBLM, including the bilateral posterior lobules VI, VIII, Crus I and the bilateral dentate nucleus, bilateral anterior lobules IV-V, and vermis lobules IV-V, and in the bilateral dorsal medial nucleus of the thalamus (MD). Increased VIM-related FC was observed in the bilateral primary and supplementary MC. The details of the cluster sizes, *T*-values and peak MNI coordinates are listed in Table II.

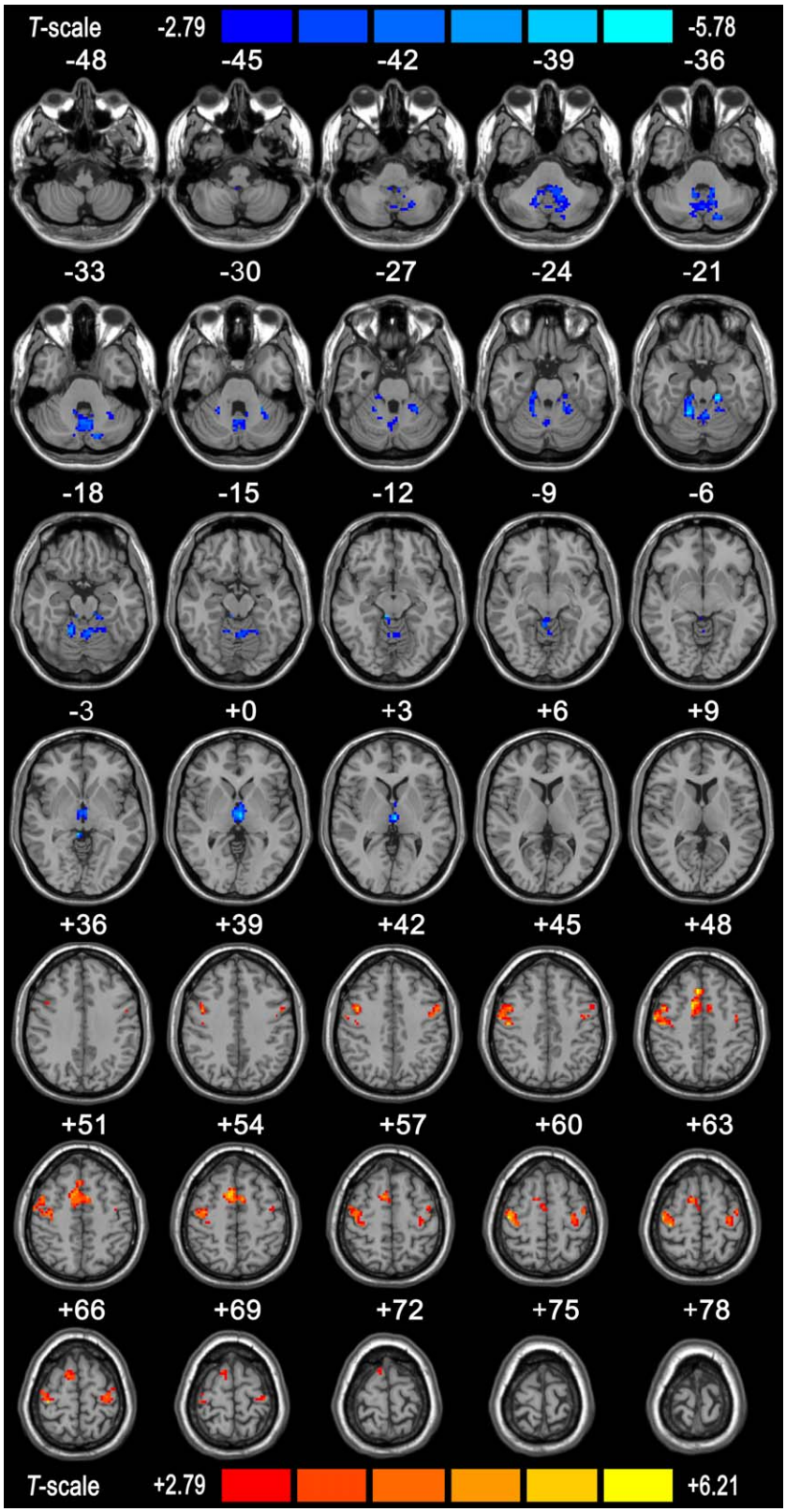

Figure 3.

Difference in left VIM seed region FC between the ET patient and HC groups. The results were obtained using the two-tailed two-sample *t* test within a combined one-sample *t*-test mask ($P < 0.01$, AlphaSim corrected with a cluster size of ≥ 10 voxels, 1000 Monte Carlo simulations). Regions displaying increased FC in the ET patients compared with the HCs are indicated by warm colors, whereas those displaying decreased FC in the ET patients are indicated by cold colors. The *Ch2* image shows the underlying structure. VIM: ventral intermediate nucleus; FC: functional connectivity; ET: essential tremor; HCs: healthy controls. [Color figure can be viewed in the online issue, which is available at wileyonlinelibrary.com.]

TABLE II. Differences in Left VIM seed FC between ET patients and HCs

Brain region	Voxels size	*T*-value	MNI coordinates		
			x	*y*	*z*
Cluster 1 (Peak MNI: 16 −59 −42, P = 0.01, corrected) Voxels size:634					
Cerebellum posterior Lobe					
Right cerebellum VI	87	−4.86	26	−55	−26
Right cerebellum Crus 1	96	−3.75	32	−66	−29
Vermis IV V	45	−2.83	−1	−50	−17
Vermis VI	37	−4.38	−4	−62	−17
Right cerebellum VIII and detnate	134	−4.25	−14	−55	−39
Left cerebellum VIII and detnate	115	−5.27	16	−59	−39
Cluster 2 (Peak MNI: 16 −45 −21, *P* = 0.01, corrected) Voxels size:321					
Cerebellum anterior Lobe					
Right cerebellum IV–V	115	−5.65	16	−47	−21
Left cerebellum IV–V	163	−5.32	−11	−44	−23
Cluster 3 (Peak MNI: 3 − 18 − 1, *P* = 0.01, corrected) Voxels size:75					
Right cerebrum					
Right thalamus					
Left thalamus					
Right medial dorsal nucleus	13	−4.78	−3	−16	−1
Left medial dorsal nucleus	26	−4.25	2	−13	3
Cluster 4 (Peak MNI: −34 − 26 60, *P* = 0.01, corrected) Voxels size:581					
Right Precentral	109	6.15	40	−16	56
Left Precentral	132	5.24	−34	−24	62
Right supplementary motor cortices	127	5.34	10	8	49
Left supplementary motor cortices	145	4.26	−5	3	54

VIM: ventral intermediate nucleus; FC: functional connectivity; ET: essential tremor; HCs: healthy controls; MNI: Montreal neurological institute.

Imaging Results-Behavior Correlation

Eight clusters displaying significant between-group differences were detected, and 8 ROIs were defined. Correlation analyses between the mean FC values for each ROI and the clinical assessment data were performed. Significant correlations were detected between 6 out of the 8 ROIs and the TRS parts A&B scores. However, there were no significant correlations between the other ROIs and the other clinical assessment parameters, including the TRS part C scores, age at onset and disease duration. Specifically, significantly negative correlations were noted between the TRS parts A&B scores and the mean FC values for the bilateral anterior cerebellar lobules (peak MNI coordinates for right: $x = 16$, $y = -47$, $z = -21$, $r = -0.44$; left: $x = -11$, $y = -44$, $z = -23$, $r = -0.53$, $P < 0.01$, uncorrected) and the bilateral posterior lobules (peak MNI coordinates for right: $x = 16$, $y = -59$, $z = -39$, $r = -0.51$; left: $x = -14$, $y = -55$, $z = -39$, $r = -0.62$, $P < 0.01$, uncorrected). A significant positive correlation was observed between the TRS parts A&B scores and the mean FC values for the bilateral primary MC (peak MNI coordinates for right: $x = 40$, $y = -16$, $z = 56$, $r = 0.49$; left: $x = -34$, $y = -24$, $z = 62$, $r = 0.57$, $P < 0.01$, uncorrected; scatter plots of these relationships are shown in Fig. 4A,B).

Spatial Specificity Evaluation of the VIM Seed Region

Figure 1B summarizes the ROI-wise partial RS-FC results. The ANOVA results showed that the partial FC values were significantly different between the ipsilateral primary MC and our five seed regions located in the ventrolateral thalamus, including the VIM (ROI_3) and four other ventral lateral thalamic nuclei (ROI_1, ROI_2, ROI_4, and ROI_5; $P < 0.05$, corrected). Post hoc *t*-tests further revealed significantly increased partial FC values between the VIM seed region and the ipsilateral primary MC in the ET patients ($P < 0.05$, corrected).

DISCUSSION

To the best of our knowledge, this study is the first to investigate the VIM FC network of RS-fMRI at the whole-brain level in ET patients, and we obtained four novel findings. First, the ET patients and the HCs shared similar VIM FC networks that were mainly composed of a VIM - MC - CBLM circuit and that also extended to the basal ganglia, the brainstem and other thalamic nuclei. Second, compared with those in the HCs, the VIM-related FC changes in the ET patients were primarily localized within

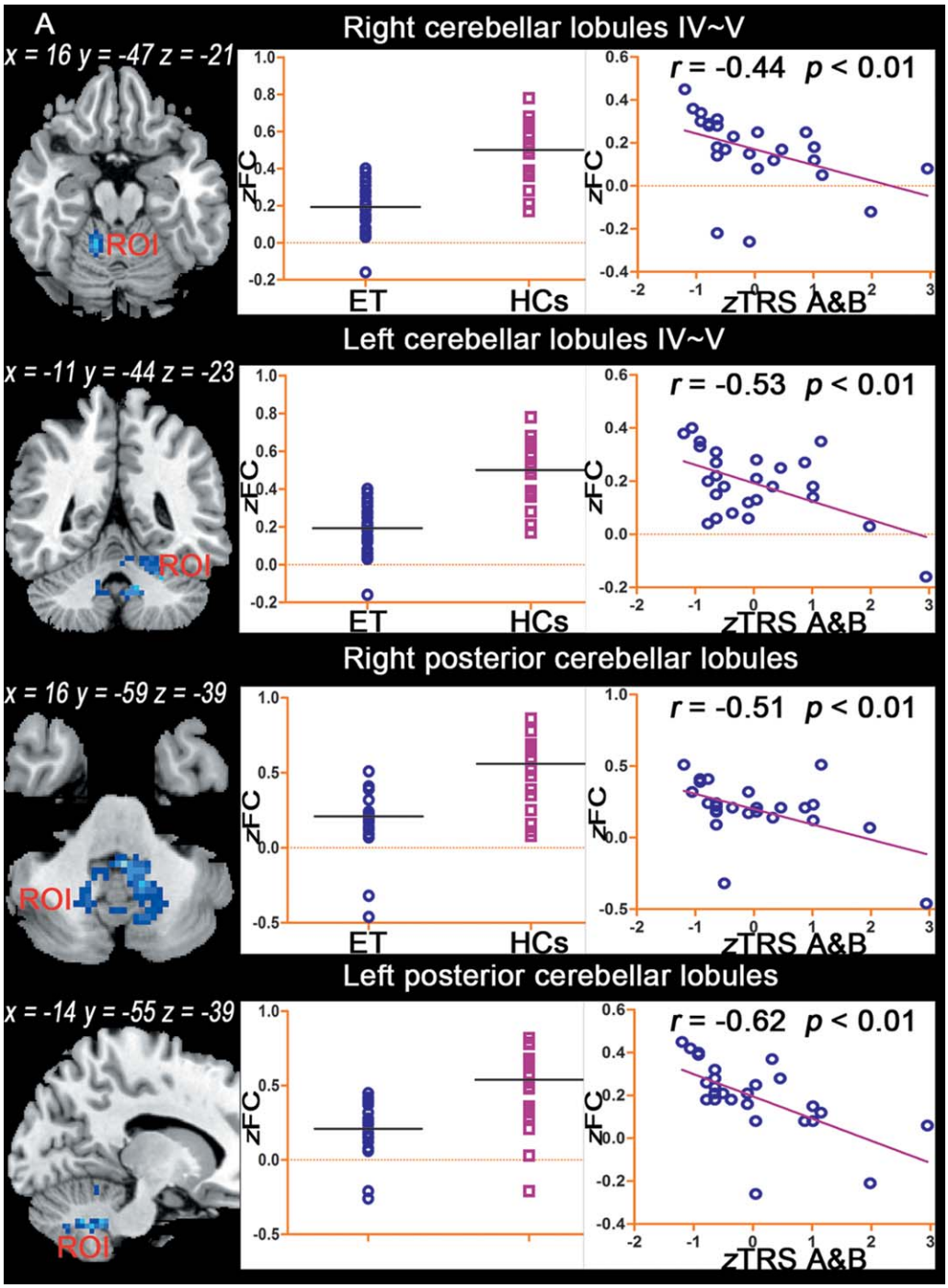

Figure 4.

Imaging results-behavior correlation analysis. The left panel shows the location of the ROIs, as determined by the two-sample *t*-test. The clusters displaying altered FC in essential tremor (ET) patients were identified as the ROIs. The middle panel shows the average FC values in each ROI for the ET patient and HC groups. The right panel shows the scatter plots of the mean FC value for each ET patient against the corresponding *z* score of the TRS parts A&B scores ($P < 0.01$, uncorrected). TRS parts A&B scores: the combined Fahn-Tolosa-Marin TRS parts A and B scores, zFC: Fisher's z-transformation of FC. [Color figure can be viewed in the online issue, which is available at wileyonlinelibrary.com.]

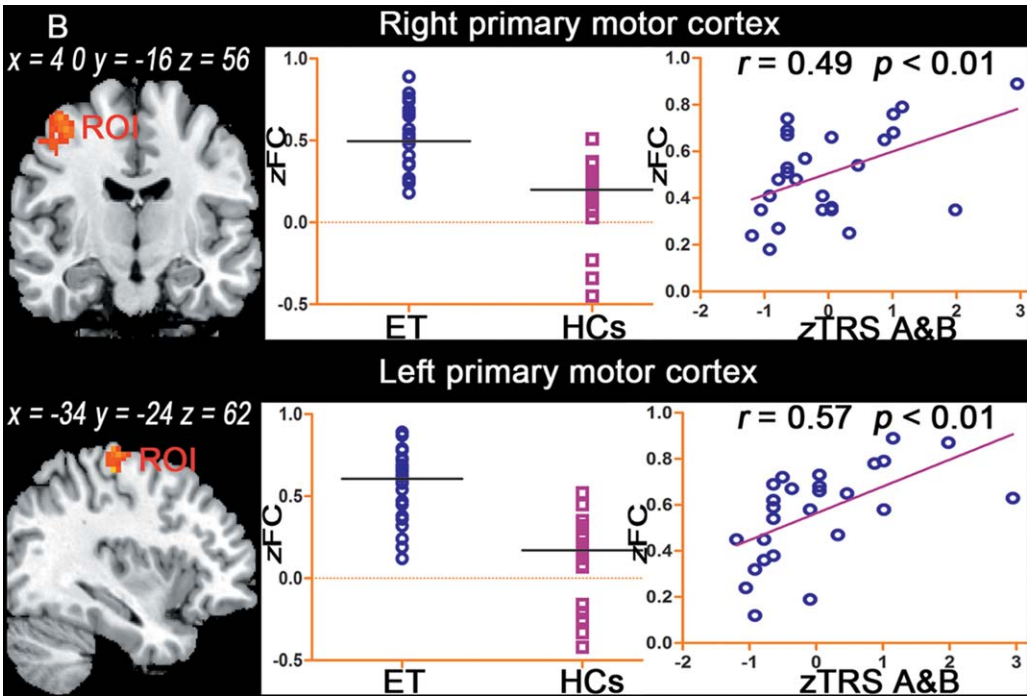

Figure 4.
(Continued).

the VIM - MC - CBLM circuit, included decreased FC in the CBLM and increased FC in the MC. Third, FC changes in this circuit correlated with tremor severity. Fourth, VIM-related FC changes in the MD, which is not a component of this circuit, were detected. The following discussion is focused on the main findings with regard to the tremor network in ET patients.

The VIM - MC - CBLM Circuit Is Not an Intrinsically Pathological Tremor Network in ET Patients

The principal features of the VIM FC maps constructed for the ET patients (Fig. 2) showed that the FC network was primarily composed of a VIM - MC - CBLM circuit. Considering the previously reported clinical benefits of VIM targeting for the treatment of tremors and the association of disrupted VIM-related FC in the CBLM and the MC with tremor severity in our study (Fig. 4), this circuit may represent an intrinsically pathological tremor network in ET patients. However, prior studies have shown that this circuit is an anatomical connectivity network in normal nonhuman primates [Asanuma et al., 1983a; Yamamoto et al., 1983] and healthy humans [Behrens et al., 2003; Johansen-Berg et al., 2005; Kincses et al., 2012]. Second, brain activity modulations are observed in this circuit during a physiological tremor task in normal non-human primates [Yamamoto et al., 1983] and healthy humans [Pollok et al., 2004]. Again, The VIM - MC - CBLM circuit participates in tremor generation and propagation in patients with PD [Helmich et al., 2011], another disease with tremor symptoms. Additionally, the HCs in our study exhibited a similar FC network to that of the ET patients. All of these findings suggest that this circuit is not an intrinsically pathological tremor network in ET patients, but rather that the pathological tremors observed in ET are attributed to a physiologically pre-existing VIM - MC - CBLM network.

Disruption of FC In the VIM - MC - CBLM Circuit Is Associated with Tremors in ET

The between-group comparisons (Fig. 3) showed that the VIM-related FC changes in the ET patients were primarily localized within the VIM - MC - CBLM circuit. These FC changes, which included decreased FC in the CBLM and increased FC in the MC, were correlated with tremor severity (Fig. 4A,B). It remains under debate whether the CBLM is involved in tremor generation and propagation in ET patients, and the most controversial findings have been reported by histopathological studies [Hallett, 2014; Jellinger, 2014]. Very few studies [Jellinger, 2014; Louis, 2014] have shown that loss of Purkinje cells and changes in Purkinje cell morphology, including in the

axonal and dendritic compartments, such as axonal swelling (torpedoes), thickened axonal profiles, increased recurrent axonal collaterals, axonal sprouting, and dendritic swelling, are tissue-specific pathological characteristics of ET. However, other studies [Rajput et al., 2011, 2012] have not found loss of Purkinje cells in ET patients. Due to the very low autopsy rate of ET patients, noninvasive methods are the primary tools used to explore the pathophysiological mechanisms underlying ET. Neuroimaging studies have noted that gray matter atrophy [Bagepally et al., 2011], white matter microstructural deficits [Klein et al., 2011], abnormal cerebral blood flow [Perlmutter et al., 2002] and hyperactivity [Bucher et al., 1997] of the CBLM are associated with tremors in ET. Additionally, a wide range of clinical observations [Louis, 2014; Stolze et al., 2001] have demonstrated that various additional motor deficits in ET patients, such as ataxia, balance and gait disorders, impaired hand-reaching function and intention tremor, are linked to cerebellar dysfunction. Taken together, all of these findings support the notion that the CBLM plays a key role in tremor generation and propagation in ET patients.

Additionally, the between-group comparisons revealed that the VIM-related FC changes in ET patients involved the MC. Electrophysiology studies [Raethjen and Deuschl, 2012; Shibasaki, 2012] have shown that the MC generates voluntary physiological movements and involuntary pathological movements, including tremors in ET patients. Moro et al. [2011] have reported that DBS of the subdural MC alleviates tremors in ET patients. However, histopathological [Louis, 2014], and microstructural [Klein et al., 2011] studies and experiments using animal models [Elble, 1998] have not revealed any abnormalities in the MC of ET patients or models. Therefore, the findings of our study support the notion that the MC is an important node of the VIM - MC - CBLM network and that tremors in ET patients may be driven by disruption of FC in this network.

VIM-Related FC Changes in MD May Be Associated with non-Motor Symptoms in ET Patients

The VIM-related FC network identified in our study was not confined to the VIM - MC - CBLM circuit; rather, it extended into other brain regions, such as the basal ganglia, the brainstem, and other thalamic nuclei. In particular, the MD displayed differences in VIM-related FC between the ET patients and the HCs. Interpretation of these findings is challenging because the VIM-related FC network is not completely consistent with the VIM-related anatomical network and because the MD is not associated with any motor function or with tremors. A functional network is ultimately determined by its structural network. However, functional networks are more complex than structural networks [Biswal, 2012; Zhang et al., 2010]. This phenomenon may plausibly explain why the VIM FC network was not completely confined to the VIM - MC - CBLM anatomical circuit. The MD is widely regarded as an important structure of the thalamus that mediates cognitive function [Schmahmann and Pandya, 2008]. Previous studies [Fields et al., 2003; Lucas et al., 2000] have reported that DBS of the VIM not only alleviates tremor symptoms but also influences cognitive function in ET patients. Cytoarchitectural and electrophysiological studies [Hernandez et al., 2015] have shown that reticular cells provide the structural and functional basis for interconnections among these nuclei in the thalamus. Therefore, we suggest that VIM-related FC changes in the MD may provide further evidence for understanding the mechanisms by which DBS of the VIM influences cognitive function in ET.

Limitations Future Directions

Although the VIM-related FC networks identified in the ET patients and the HCs are highly consistent with the individual anatomical connectivity networks revealed by invasive tract-tracing and noninvasive DTI studies of normal non-human primates [Asanuma et al., 1983a; Yamamoto et al., 1983] and healthy humans [Behrens et al., 2003; Johansen-Berg et al., 2005; Kincses et al., 2012], we must use caution when interpreting these findings, especially when applying them at an individual level. Additionally, to reveal the characteristic profiles of ET, a homogenous entity is necessary because growing evidence has suggested that ET is not a single disease but rather is a family of diseases or a syndrome [Louis et al., 2014]. In our study, all ET patients presented with kinetic tremors in their hands and arms as their main clinical features, and without a tremor onset after age 65 years. Thus, in these patients, ET appeared to be a homogenous entity. However, stringent tremor severity thresholds were not adopted, which would have made our ET patient cohort more representative [Louis, 2015; Louis et al., 2014]. In the future, the adoption of stringent tremor severity thresholds, such as hand-drawn spiral rating ≥ 1.5 [Louis, 2015] or kinetic tremor rating ≥ 2 during three or more hands functional tests [Louis et al., 2014], may produce more representative and reproducible results.

CONCLUSIONS

The results of FC analysis of RS-fMRI data in combination with previous findings provide evidence that ET patients and HCs share the same VIM-related RS-FC network and that this network is highly consistent with the anatomical connectivity network. Further, our findings suggest that the pathological tremors observed in ET patients might be associated with a physiologically preexisting VIM - MC - CBLM network and that disruption of FC in this physiological network is associated with ET.

ACKNOWLEDGMENTS

Contract grant sponsor: Natural Science Foundation of Chongqing; Contract grant number: cstc2014jcyjA10047; Contract grant sponsor: Medicine Scientific Key Research Project of Chongqing Health Bureau (Project No. 2010-2-030); Contract grant sponsor: National Natural Science Foundation of China; Contract grant number: 81201156

REFERENCES

Anderson JS, Dhatt HS, Ferguson MA, Lopez-Larson M, Schrock LE, House PA, Yurgelun-Todd D (2011): Functional connectivity targeting for deep brain stimulation in essential tremor. AJNR Am J Neuroradiol 32:1963–1968.

Asanuma C, Thach W, Jones E (1983a): Distribution of cerebellar terminations and their relation to other afferent terminations in the ventral lateral thalamic region of the monkey. Brain Res Rev 5:237–265.

Asanuma C, Thach WT, Jones EG (1983b): Cytoarchitectonic delineation of the ventral lateral thalamic region in the monkey. Brain Res 286:219–235.

Bagepally BS, Bhatt MD, Chandran V, Saini J, Bharath RD, Vasudev M, Prasad C, Yadav R, Pal PK (2011): Decrease in Cerebral and Cerebellar Gray Matter in Essential Tremor: A Voxel-Based Morphometric Analysis under 3T MRI. J Neuroimaging 22:275–278.

Behrens T, Johansen-Berg H, Woolrich M, Smith S, Wheeler-Kingshott C, Boulby P, Barker G, Sillery E, Sheehan K, Ciccarelli O (2003): Non-invasive mapping of connections between human thalamus and cortex using diffusion imaging. Nat Neurosci 6:750–757.

Bernard JA, Peltier SJ, Benson BL, Wiggins JL, Jaeggi SM, Buschkuehl M, Jonides J, Monk CS, Seidler RD (2014): Dissociable Functional Networks of the Human Dentate Nucleus. Cereb Cortex 24:2151–2159.

Biswal BB (2012): Resting state fMRI: a personal history. Neuroimage 62:938–944.

Brittain JS, Cagnan H, Mehta AR, Saifee TA, Edwards MJ, Brown P (2015): Distinguishing the central drive to tremor in Parkinson's disease and essential tremor. J Neurosci 35:795–806.

Bucher SF, Seelos KC, Dodel RC, Reiser M, Oertel WH (1997): Activation mapping in essential tremor with functional magnetic resonance imaging. Ann Neurol 41:32–40.

Chao-Gan Y, Yu-Feng Z (2010): DPARSF: A MATLAB Toolbox for "Pipeline" Data Analysis of Resting-State fMRI. Front Syst Neurosci 4:13.

Connolly AT, Bajwa JA, Johnson MD (2012): Cortical magnetoencephalography of deep brain stimulation for the treatment of postural tremor. Brain Stimul 5:616–624.

Deuschl G, Bain P, Brin M (1998): Consensus statement of the Movement Disorder Society on Tremor. Ad Hoc Scientific Committee. Mov Disord 13:2–23.

Elble RJ (1998): Animal models of action tremor. Mov Disord 13: 35–39.

Elias WJ, Shah BB (2014): Tremor. JAMA 311:948–954.

Elias WJ, Huss D, Voss T, Loomba J, Khaled M, Zadicario E, Frysinger RC, Sperling SA, Wylie S, Monteith SJ, Druzgal J, Shah BB, Harrison M, Wintermark M (2013): A pilot study of focused ultrasound thalamotomy for essential tremor. N Engl J Med 369:640–648.

Fahn S, Tolosa E, Marin C (1993): Clinical rating scale for tremor. Parkinson's Disease and Movement Disorders 2:271–280.

Fang W, Lv F, Luo T, Cheng O, Liao W, Sheng K, Wang X, Wu F, Hu Y, Luo J, Yang QX, Zhang H (2013): Abnormal regional homogeneity in patients with essential tremor revealed by resting-state functional MRI. PLoS One 8:e69199.

Fields JA, Troster AI, Woods SP, Higginson CI, Wilkinson SB, Lyons KE, Koller WC, Pahwa R (2003): Neuropsychological and quality of life outcomes 12 months after unilateral thalamic stimulation for essential tremor. J Neurol Neurosurg Psychiatry 74:305–311.

Fox MD, Zhang D, Snyder AZ, Raichle ME (2009): The global signal and observed anticorrelated resting state brain networks. J Neurophysiol 101:3270–3283.

Hallett M (2014): Tremor: Pathophysiology. Parkinsonism Relat Disord 20:S118–S122.

Hassler R, Riechert T (1954): [Indications and localization of stereotactic brain operations]. Nervenarzt 25:441–447.

Helmich RC, Janssen MJ, Oyen WJ, Bloem BR, Toni I (2011): Pallidal dysfunction drives a cerebellothalamic circuit into Parkinson tremor. Ann Neurol 69:269–281.

Hernandez O, Hernandez L, Vera D, Santander A, Zurek E (2015): Thalamic reticular cells firing modes and its dependency on the frequency and amplitude ranges of the current stimulus. Med Biol Eng Comput 53:37–44.

Hesselmann V, Maarouf M, Hunsche S, Lasek K, Schaaf M, Krug B, Lackner K, Sturm V, Wedekind C (2006): Functional MRI for immediate monitoring stereotactic thalamotomy in a patient with essential tremor. Eur Radiol 16:2229–2233.

Hyam JA, Owen SL, Kringelbach ML, Phd NJ, Stein JF, Green AL, Aziz TZ (2012): Contrasting Connectivity of the Vim and Vop Nuclei of the Motor Thalamus Demonstrated by Probabilistic Tractography. Neurosurgery 70:162–169.

Jellinger KA (2014): Is there cerebellar pathology in essential tremor? Mov Disord 29:435–436.

Johansen-Berg H, Behrens TEJ, Sillery E, Ciccarelli O, Thompson AJ, Smith SM, Matthews PM (2005): Functional–anatomical validation and individual variation of diffusion tractography-based segmentation of the human thalamus. Cerebral Cortex 15:31–39.

Kahan J, Urner M, Moran R, Flandin G, Marreiros A, Mancini L, White M, Thornton J, Yousry T, Zrinzo L, Hariz M, Limousin P, Friston K, Foltynie T (2014): Resting state functional MRI in Parkinson's disease: The impact of deep brain stimulation on 'effective' connectivity. Brain 137:1130–1144.

Kelly C, de Zubicaray G, Di Martino A, Copland DA, Reiss PT, Klein DF, Castellanos FX, Milham MP, McMahon K (2009): L-dopa modulates functional connectivity in striatal cognitive and motor networks: a double-blind placebo-controlled study. J Neurosci 29:7364–7378.

Kincses ZT, Szabo N, Valalik I, Kopniczky Z, Dezsi L, Klivenyi P, Jenkinson M, Kiraly A, Babos M, Voros E, Barzo P, Vecsei L (2012): Target identification for stereotactic thalamotomy using diffusion tractography. PLoS One 7:e29969.

Klein JC, Lorenz B, Kang JS, Baudrexel S, Seifried C, van de Loo S, Steinmetz H, Deichmann R, Hilker R (2011): Diffusion tensor imaging of white matter involvement in essential tremor. Hum Brain Mapp 32:896–904.

Klein JC, Barbe MT, Seifried C, Baudrexel S, Runge M, Maarouf M, Gasser T, Hattingen E, Liebig T, Deichmann R, Timmermann L, Weise L, Hilker R (2012): The tremor network targeted by successful VIM deep brain stimulation in humans. Neurology 78:787–795.

Kooshkabadi A, Lunsford LD, Tonetti D, Flickinger JC, Kondziolka D (2013): Gamma Knife thalamotomy for tremor in the magnetic resonance imaging era. J Neurosurg 118:713–718.

Li SC, Schoenberg BS, Wang CC, Cheng XM, Rui DY, Bolis CL, Schoenberg DG (1985): A prevalence survey of Parkinson's disease and other movement disorders in the People's Republic of China. Arch Neurol 42:655–657.

Lin CH, Chen CM, Lu MK, Tsai CH, Chiou JC, Liao JR, Duann JR (2013): VBM Reveals Brain Volume Differences between Parkinson's Disease and Essential Tremor Patients. Front Human Neurosci 7:247

Louis ED (2014): Re-thinking the biology of essential tremor: From models to morphology. Parkinsonism Relat Disord 20(Suppl 1):S88–S93.

Louis ED (2015): Utility of the hand-drawn spiral as a tool in clinical-epidemiological research on essential tremor: Data from four essential tremor cohorts. Neuroepidemiology 44:45–50.

Louis ED, Ferreira JJ (2010): How common is the most common adult movement disorder? Update on the worldwide prevalence of essential tremor. Mov Disord 25:534–541.

Louis ED, Yousefzadeh E, Barnes LF, Yu Q, Pullman SL, Wendt KJ (2000): Validation of a portable instrument for assessing tremor severity in epidemiologic field studies. Mov Disord 15: 95–102.

Louis ED, Ottman R, Clark LN (2014): Clinical classification of borderline cases in the family study of essential tremor: An analysis of phenotypic features. Tremor Other Hyperkinet Mov (N Y), 4:220

Lucas JA, Rippeth JD, Uitti RJ, Shuster EA, Wharen RE (2000): Neuropsychological functioning in a patient with essential tremor with and without bilateral VIM stimulation. Brain Cognit 42:253–267.

Morel A, Magnin M, Jeanmonod D (1997): Multiarchitectonic and stereotactic atlas of the human thalamus. J Comp Neurol 387: 588–630.

Moro E, Schwalb JM, Piboolnurak P, Poon YYW, Hamani C, Hung SW, Arenovich T, Lang AE, Chen R, Lozano AM (2011): Unilateral subdural motor cortex stimulation improves essential tremor but not Parkinson's disease. Brain 134:2096–2105.

Murphy K, Birn RM, Handwerker DA, Jones TB, Bandettini PA (2009): The impact of global signal regression on resting state correlations: Are anti-correlated networks introduced? Neuroimage 44:893–905.

Papavassiliou E, Rau G, Heath S, Abosch A, Barbaro NM, Larson PS, Lamborn K, Starr PA (2008): Thalamic deep brain stimulation for essential tremor: relation of lead location to outcome. Neurosurgery 62: 884-894.

Perlmutter JS, Mink JW, Bastian AJ, Zackowski K, Hershey T, Miyawaki E, Koller W, Videen TO (2002): Blood flow responses to deep brain stimulation of thalamus. Neurology 58:1388–1394.

Pollok B, Gross J, Dirks M, Timmermann L, Schnitzler A (2004): The cerebral oscillatory network of voluntary tremor. J Physiol 554:871–878.

Popa T, Russo M, Vidailhet M, Roze E, Lehericy S, Bonnet C, Apartis E, Legrand AP, Marais L, Meunier S, Gallea C (2013): Cerebellar rTMS stimulation may induce prolonged clinical benefits in essential tremor, and subjacent changes in functional connectivity: an open label trial. Brain Stimul 6:175–179.

Power JD, Barnes KA, Snyder AZ, Schlaggar BL, Petersen SE (2012): Spurious but systematic correlations in functional connectivity MRI networks arise from subject motion. Neuroimage 59:2142–2154.

Power JD, Barnes KA, Snyder AZ, Schlaggar BL, Petersen SE (2013): Steps toward optimizing motion artifact removal in functional connectivity MRI; a reply to Carp. Neuroimage, 76: 439–441.

Raethjen J, Deuschl G (2012): The oscillating central network of Essential tremor. Clin Neurophysiol 123:61–64.

Rajput AH, Robinson CA, Rajput ML, Rajput A (2011): Cerebellar Purkinje cell loss is not pathognomonic of essential tremor. Parkinsonism Relat Disord 17:16–21.

Rajput AH, Robinson CA, Rajput ML, Robinson SL, Rajput A (2012): Essential tremor is not dependent upon cerebellar Purkinje cell loss. Parkinsonism Relat Disord 18:626–628.

Satterthwaite TD, Elliott MA, Gerraty RT, Ruparel K, Loughead J, Calkins ME, Eickhoff SB, Hakonarson H, Gur RC, Gur RE, Wolf DH (2013): An improved framework for confound regression and filtering for control of motion artifact in the preprocessing of resting-state functional connectivity data. Neuroimage 64:240–256.

Schmahmann JD, Pandya DN (2008): Disconnection syndromes of basal ganglia, thalamus, and cerebrocerebellar systems. Cortex 44:1037–1066.

Sheng K, Fang W, Su M, Li R, Zou D, Han Y, Wang X, Cheng O (2014): Altered spontaneous brain activity in patients with Parkinson's disease accompanied by depressive symptoms, as revealed by regional homogeneity and functional connectivity in the prefrontal-limbic system. PLoS One 9:e84705.

Shibasaki H (2012): Cortical activities associated with voluntary movements and involuntary movements. Clin Neurophysiol 123:229–243.

Snaith RP, Zigmond AS (1986): The hospital anxiety and depression scale. Br Med J (Clin Res Ed), 292:344.

Song XW, Dong ZY, Long XY, Li SF, Zuo XN, Zhu CZ, He Y, Yan CG, Zang YF (2011): REST: A toolkit for resting-state functional magnetic resonance imaging data processing. PLoS One 6:e25031.

Stolze H, Petersen G, Raethjen J, Wenzelburger R, Deuschl G (2001): The gait disorder of advanced essential tremor. Brain 124:2278.

Van Dijk KR, Sabuncu MR, Buckner RL (2012): The influence of head motion on intrinsic functional connectivity MRI. Neuroimage 59:431–438.

Vassal F, Coste J, Derost P, Mendes V, Gabrillargues J, Nuti C, Durif F, Lemaire JJ (2012): Direct stereotactic targeting of the ventrointermediate nucleus of the thalamus based on anatomic 1.5-T MRI mapping with a white matter attenuated inversion recovery (WAIR) sequence. Brain Stimul 5:625–633.

Werner CJ, Dogan I, Sass C, Mirzazade S, Schiefer J, Shah NJ, Schulz JB, Reetz K (2014): Altered resting-state connectivity in Huntington's Disease. Hum Brain Mapp 35:2582–2593.

Wintermark, M, Huss, DS, Shah, BB, Tustison, N, Druzgal, TJ, Kassell, N, Elias, WJ (2014): Thalamic Connectivity in Patients with Essential Tremor Treated with MR Imaging-guided Focused Ultrasound: In Vivo Fiber Tracking by Using Diffusion-Tensor MR Imaging. Radiology 272:202–209.

Yamamoto T, Wagner A, Hassler R, Sasaki K (1983): Studies on the cerebellocerebral and thalamocortical projections in squirrel monkeys (Saimiri sciureus). Exp Neurol 79:27–37.

Zhang D, Snyder AZ, Fox MD, Sansbury MW, Shimony JS, Raichle ME (2008): Intrinsic functional relations between human cerebral cortex and thalamus. J Neurophysiol 100:1740–1748.

Zhang D, Snyder AZ, Shimony JS, Fox MD, Raichle ME (2010): Noninvasive functional and structural connectivity mapping of the human thalamocortical system. Cerebral Cortex 20:1187–1194.

Zhang MY, Katzman R, Salmon D, Jin H, Cai GJ, Wang ZY, Qu GY, Grant I, Yu E, Levy P (1990): The prevalence of dementia and Alzheimer's disease in Shanghai, China: Impact of age, gender, and education. Ann Neurol 27:428–437.

Zirh A, Reich S, Dougherty P, Lenz F (1999): Stereotactic thalamotomy in the treatment of essential tremor of the upper extremity: Reassessment including a blinded measure of outcome. J Neurol Neurosurg Psychiatry 66:772–775.